Thermodynamic Study of the Effects of Ursodeoxycholic Acid and Ursodeoxycholate on Aqueous Dipalmitoyl Phosphatidylcholine Bilayer Dispersions†

Maria Tomoaia-Cotisel‡ and Ira W. Levin*

Laboratory of Chemical Physics, National Institute of Diabetes and Digestive and Kidney Diseases, National Institutes of Health, Bethesda, Maryland 20892

Received: March 19, 1997; In Final Form: June 24, 1997⊗

The effects of ursodeoxycholic acid (UDCAH) and ursodeoxycholate ($UDCA^-$) on the thermotropic phase behavior of aqueous bilayer dispersions of 1,2-dipalmitoyl-3-*sn*-phosphatidylcholine (DPPC), buffered at pH 7.0, were examined by differential scanning calorimetry (DSC) for concentrations of UDCAH and $UDCA^-$ (represented by UDCA) from 0 to approximately 76 mol %. The calorimetric data show that progressively increasing UDCA concentrations decreases the DPPC bilayer main transition temperatures (T_m), while increasing the widths of the gel to liquid crystalline phase transition endotherms. The DPPC bilayer pretransition is suppressed in the presence of UDCA at the lowest concentrations employed. The calorimetric data, which are interpreted in terms of the partition equilibria of UDCAH and $UDCA^-$ and of the DPPC bilayer phase transition enthalpies and Gibbs free energies, allow the development of a thermodynamic approach for determining the phase boundaries in mixed DPPC:UDCA dispersions. In particular, for concentrations of UDCA up to approximately 25 mol %, the gel to liquid crystalline phase transition enthalpies of the mixed DPPC:UDCA bilayers remain essentially constant. The increase that occurs in the DPPC gel to liquid crystalline phase transition enthalpies for UDCA concentrations between approximately 25−60 mol % is interpreted in terms of an induced interdigitated gel (L_{gI}) phase stabilized by specific DPPC:UDCA molecular interactions. The data suggest that the interdigitated gel phase exists in equilibrium with micelles, whose structures remain to be elucidated, of various UDCA:DPPC mole ratios. Finally, concentrations of UDCA in amounts greater than 60 mol % result in constant DPPC phase transition temperatures and enthalpies.

Introduction

Thermodynamic studies of mixed aqueous dispersions containing bile acids, bile salts, and lipids are useful both for understanding, in general, the self-assembling properties of biological aggregates and for elucidating the phase and interfacial behavior of these surfactants. Extensive research has focused on the effects of a variety of bile acids, bile salts, and their conjugates on lipid bilayers[1−16] using diverse experimental techniques including light scattering,[3,7,15] calorimetry,[4,11] small-angle X-ray scattering,[5] nuclear magnetic resonance spectroscopy,[6] absorbance titrations,[9] turbidity,[10] and small-angle neutron scattering.[12−14] These studies demonstrate the sensitivity of the phase behavior of the mixed dispersions to molecular composition and emphasize the unique physical and chemical properties assumed by self-assembled lipid aggregates in the presence of either a bile salt or bile acid. Examination of the various phase transitions available to these assemblies provide information on the structural transformations between phases of differing compositions and aggregation geometries.

Bile acids, and in particular, ursodeoxycholic acid (3α,7β-dihydroxy-5β-cholan-24-oic acid or UDCAH), are fundamentally important in a variety of biological and biomedical areas.[8,17,18] In recent years, for example, ursodeoxycholic acid, ursodeoxycholate ($UCDA^-$), and their conjugates have been utilized, either alone or in combination, in the treatment of various liver and related diseases.[19,20] Despite the existence of a relatively large compilations of data on the biochemical, physiological, and clinical aspects of UDCAH and $UDCA^-$ (representing both species by UDCA) and on their therapeutic efficacy,[8,17−20] a detailed quantitative knowledge of the physical and chemical properties of mixed UDCA:lipid dispersions is not generally accessible.

In the present study we investigate mixed UDCA:lipid dispersions at pH 7.0 by differential scanning calorimetry (DSC), a technique widely used in studying the phase behavior of liposomal assemblies. 1,2-Dipalmitoyl-*sn*-glycero-3-phosphocholine (DPPC) was chosen as the lipid substrate since the thermotropic properties leading to various lipid phase bilayer structures are well established; that is, for the pure system the sequence of the lamellar crystalline (L_c), lamellar gel ($L_{\beta'}$), rippled gel ($P_{\beta'}$), and liquid crystalline (L_α) phases has been well characterized as functions of temperature.[21−25] This report focuses specifically on the phase behavior of DPPC bilayers in the presence of UDCA and attempts to obtain quantitative data for gaining insight into the potential roles of UDCA:phospholipid assemblies in regulating membrane function. By characterizing thermodynamically these mixed UDCA:DPPC dispersions, one is able to detail the classes of molecular aggregates induced by these bile species both within different bilayer phase structures and within membrane microdomains. For example, on the basis of the calorimetric data, we suggest the existence of an interdigitated, or partially interdigitated, lipid chain phase for systems containing UDCA within a specified concentration range. This interdigitated phase, an example of a composition driven structural transition, is often induced by the action of amphiphillic compounds and is accompanied by readjustments in the packing properties of the lipid molecules within the bilayer.[26−31] Finally, we are interested in the biophysical

† This work was presented in part at the XIII International Bile Acid Meeting, Bile Acids in Gastroenterology: Basic and Clinical Advances, 1994, San Diego, CA, and published as an abstract in the Falk Symposium, No. 80, 1994.

* To whom correspondence should be addressed.

‡ Present address: Molecular/Structural Biotechnologies, Inc., 3 Bethesda Metro Center, Bethesda, MD 20814.

⊗ Abstract published in *Advance ACS Abstracts,* October 1, 1997.

S1089-5647(97)00990-5

implications raised in studies of the effects of UDCA on the interfacial energetics of lipid membranes, particularly with respect to the ordering properties of the bilayer core in different phases of the system and to the role of interaction forces in stabilizing UDCA:phospholipid structures.

Experimental Section

(A) Materials. Synthetic 1,2-dipalmitoyl-*sn*-glycero-3-phosphocholine (DPPC: 1,2-dipalmitoyl-3-*sn*-phosphatidylcholine) was purchased from Avanti Polar Lipids, Inc. Ursodeoxycholic acid (UDCAH: 3α,7β-dihydroxy-5β-cholan-24-oic acid) was purchased from Sigma Chemical Co. Both compounds were used without further purification. Standard buffer solutions of pH 7.00 ± 0.01 at 25 °C were obtained from Mallinckrodt Chemical, Inc., and from Fisher Scientific (e.g., buffer containing potassium phosphate monobasic and sodium hydroxide). Also standard buffers of pH 4.00± 0.01 and 10.00 ± 0.01 at 25 °C were purchased from Fisher Scientific. All chemicals and organic solvents were of analytical and of spectroscopic grades, respectively.

(B) Solutions and Dispersions. Appropriate amounts of either DPPC or of samples of DPPC and UDCAH at various mole ratios were dissolved in chloroform or in mixtures of chloroform:methanol (3:2, v/v) and then dried to thin films in glass tubes by gently blowing purified dry (99.99%) nitrogen across the samples for 12−24 h. After the samples were further dried under high vacuum to constant weight, the resultant films were hydrated with a standard phosphate buffer (pH 7.0) at 65 °C, well above the DPPC main gel to liquid crystalline phase transition temperature of 41.3 °C for at least 1 h. The DPPC concentrations of the final aqueous dispersions were approximately 0.01 M. During this incubation period, the samples were mechanically agitated until a uniform homogeneous dispersion was obtained. Each sample was cycled 20 times through the main phase transition (heating and cooling) to ensure an equilibrated and fully hydrated system. Typically, no change was observed in the calorimetric thermograms after the fifth sample heating and cooling cycle, although each sample was subjected routinely to 20 cycles before recording calorimetric data. All lipid/bile acid dispersions were incubated for at least 1 day at 4 °C and for 1 week at −14 °C prior to recording calorimetric traces. Since the phase transition behavior of DPPC is dependent on the details of the preparation of the lipid dispersions,[24,25] uniform experimental procedures, as described above, were imposed to ensure the consistency of the measured phase transition enthalpies.

Although the DPPC concentration employed was much higher than that required on the basis of the sensitivity of the calorimeter, these high lipid concentrations were used in order to ensure flat base lines for the accurate determinations of the onset ($T_{onset} = T_B$) and completion ($T_{completion} = T_E$) temperatures of the thermal transitions. The difference between these two temperatures provides the width of the phase transition, a measure of phase transition cooperativity.

The H^+ ion activities (in terms of pH values) were measured with a research pH meter and a H^+ sensitive glass electrode. The pH-meter was calibrated at pH 4.00 ± 0.01 and 10.00 ± 0.01 with standard buffers. All DPPC dispersions in the absence and in the presence of UDCAH were prepared in standard phosphate buffers of pH 7.00 ± 0.01. The pH of all dispersions, measured both before and after the calorimetric measurements, indicated that no pH changes occurred during the recording of the data.

(C) Differential Scanning Calorimetry (DSC). DSC curves were performed on a Hart-Scientific, Inc., Model 707 series differential scanning calorimeter equipped for computer control of data acquisition and subsequent analysis.[52] Instrumental base lines were obtained by scanning either buffer solutions or doubly distilled and deionized water in both the sample and reference cells of the calorimeter. These base lines were horizontal over the temperature range (288−333 K) of interest. The DSC measurements performed with blank UDCA dispersions at pH 7.0 showed no thermotropic behavior for the pure UDCA dispersions over the 288−333 K temperature range. Approximately 0.5 mL of each DPPC dispersion, in the absence or in the presence of UDCA, and the corresponding buffer or blank were loaded into the calorimeter sample and reference cells, respectively. The sample and buffer, or blank, cells were allowed to reach thermal equilibrium, generally within 2 h, prior to the initiation of a scan. Scans were generally recorded from 288 to 333 K at a heating rate of 10 °C/hr (i.e., approximately 0.16 °C/min). As a check on reproducibility, a number of scans were performed with a heating rate of 5 °C/hr (about 0.08 °C/min). Since the experimental DSC curves for all systems were independent of the heating rate, a scan rate of 0.16 °C/min was chosen to ensure precise equilibrium heat measurements.

Three DSC runs were recorded for ascending temperatures for each lipid:UDCA composition. Rescanning samples provided DSC curves identical with the first scan, indicating that no substantial lipid decomposition took place during the heating runs. The reversible nature of the phase transitions, indicated by the reproducibility of the DSC curves, demonstrated that all dispersions were in equilibrium. The phase transition temperature T_m for each composition was determined by averaging multiple runs with T_m being determined from the midpoint temperature, or the temperature of maximal heat absorption, of the averaged endotherms. The pretransition temperature T_p was determined similarly. Analysis of the calorimetric data, employing the software supplied by Hart Scientific, Inc., yielded both the biosurfactant excess heat flow as a function of temperature and bilayer transition enthalpy. Base line corrections and the relative excess heat curves for all dispersions, calculated by normalizing the experimental averaged DSC curve of each dispersion to the pure DPPC dispersion (DPPC concentration being almost constant, around 10×10^{-3} mol/L, in each dispersion) were performed with laboratory software. The DSC data were analyzed in terms of a two-state phase transition model for DPPC bilayers.[24,25]

Results and Discussion

I. Molecular Species Involved. UDCAH participates in dissociation equilibria in which the degree of UDCAH ionization is sensitive to the pH of the environment. Since the physiological function of UDCAH is dependent on the degree of its ionization, the acidity constant K_a of UDCAH in bulk dispersions has been a subject of long term interest[32−34] with an apparent pK_a value being determined to be approximately 5.1. We assume in our discussion that the acidity constant (K'_a) of UDCAH in association (incorporated or adsorbed) with the DPPC bilayers is equivalent to its K_a value. This approximation has been used for various drugs bound to DPPC bilayers.[35] Since we performed experiments on dispersions buffered to pH 7.0, near physiological pH, approximately 1% of the initial UDCAH exists as the free acid (UDCAH) at this pH, while the remaining 99% exists in its anionic form ($UDCA^-$). For simplicity, we express the total concentration, symbolized as UDCA, in terms of all molecular species (UDCAH and $UDCA^-$) in each dispersion; that is, the total number of moles given by the sum $n_{UDCAH} + n_{UDCA^-}$, with the anion as the dominant species, is denoted as n_{UDCA}.

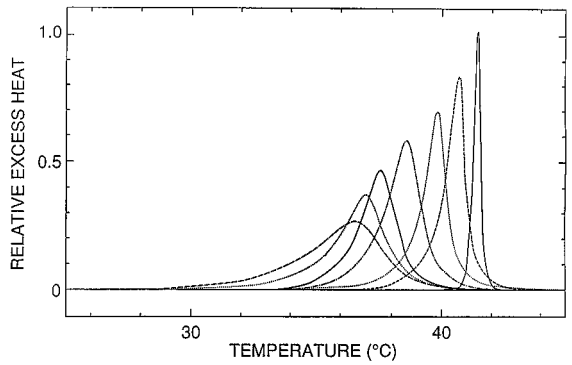

Figure 1. DSC thermograms of DPPC dispersions (heating mode) in the absence (solid curve, at right) and in the presence of increasing concentrations of UDCA at pH 7. Symbols: solid line, $X_{DPPC} = 1.000$; dashed, 0.946; dotted, 0.915; dot−dashed, 0.825; solid, 0.724; dotted, 0.658; dashed, 0.525.

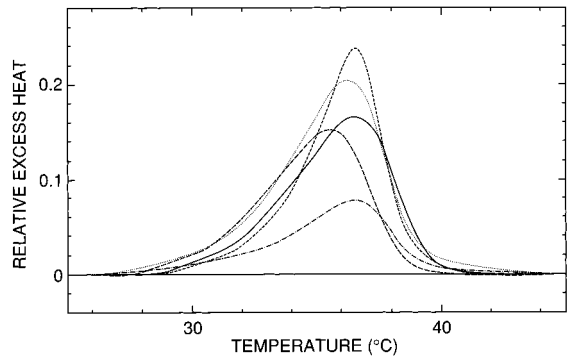

Figure 2. Endotherms of DPPC:UDCA dispersions at pH 7 of compositions expressed in mole fraction of DPPC. Symbols: short dashed, $X_{DPPC} = 0.500$; dotted, 0.460; solid, 0.400; long dashed, 0.356; dot−dashed, 0.235.

II. Endothermic DSC Curves. Representations of the DSC endotherms, expressed in terms of the relative excess heat versus temperature, of DPPC bilayers containing increasing concentrations of UDCA are given in Figures 1 and 2. The composition is expressed as a mole fraction of DPPC, noted as $X_{DPPC} = n_{DPPC}/(n_{DPPC} + n_{UDCA})$, where n_i is the total number of moles of component i in the mixed dispersions. Similarly, X_{UDCA} represents the total mole fraction of bile acid and its salt, and $X_{UDCA} + X_{DPPC} = 1$. All mole fractions are based on the total amount of bile acid (UDCAH) initially introduced into the sample.

In the absence of UDCA, the thermogram is characterized by a sharp peak at $T_m^\circ = 314.50 \pm 0.05$ K (Figure 1 and Table 1), which is associated with a reversible gel to liquid crystalline phase transition of pure DPPC multilamellar bilayer dispersions. This main phase transition, attributed to the $P_{\beta'}$ rippled gel to L_α liquid crystalline phase transition of pure DPPC bilayers, has been exhaustively studied.[21−25,36,37] The phase transition enthalpy (ΔH°_{DPPC}) of 8.5 ± 0.1 kcal/mol (Table 3) is consistent with the average value of 8.3 kcal/mol reported from DSC measurements.[25] This value of ΔH°_{DPPC} is also similar to those found for pure DPPC multilamellar bilayer dispersions [21−25,36,37] and is related primarily to the chain melting, or disordering, within the pure DPPC bilayers. The estimated half-height width for this sharp transition reproducibly yields values between 0.17 and 0.20 K (Figure 1), which agrees well with other reported values [24,25,37] and reflects the high cooperativity of the melting phenomenon. The pure DPPC bilayer thermogram also exhibits a second broad peak at a lower temperature $T_p^\circ = 308.48 \pm 0.25$ K, with an associated $\Delta H^\circ_{p,DPPC} = 1.5 \pm 0.3$ kcal/mol, which is in good agreement with other reported values.[21−25,29]

TABLE 1: Thermotropic Phase Transitions Exhibited by Aqueous Dispersions of DPPC and UDCA at pH 7

sample	main transition temperature (T_m) (K)		
X_{UDCA}	gel/L_α	L_{gI}/L_α	$L_{g'}/L_\alpha$
0.000	314.50 ± 0.05		
0.054	313.70 ± 0.07		
0.065	313.50 ± 0.08		
0.085	313.11 ± 0.09		
0.125	312.60 ± 0.09		
0.150	312.18 ± 0.08		
0.175	311.70 ± 0.09		
0.210	311.40 ± 0.10		
0.240	310.85 ± 0.10		
0.276		310.73 ± 0.11	
0.287		310.60 ± 0.10	
0.300		310.55 ± 0.12	
0.342		310.30 ± 0.10	
0.425		309.91 ± 0.09	
0.475		309.65 ± 0.10	
0.500		309.55 ± 0.10	
0.512		309.45 ± 0.09	
0.535		309.25 ± 0.11	
0.540		309.35 ± 0.12	
0.600			309.29 ± 0.20
0.644			308.95 ± 0.22
0.765			309.22 ± 0.25

TABLE 2: Effect of UDCA Incorporation on the Main Transition Temperature T_m of DPPC Dispersions at pH 7

	$T_{onset} = T_B$ (K)			$T_{completion} = T_E$ (K)		
X_{UDCA}	gel/L_α	L_{gI}/L_α	$L_{g'}/L_\alpha$	gel/L_α	L_{gI}/L_α	$L_{g'}/L_\alpha$
0.000	314.32			314.77		
0.054	312.90			314.35		
0.065	312.85			314.20		
0.085	312.40			314.15		
0.125	311.40			313.70		
0.150	310.65			313.55		
0.175	310.04			313.15		
0.210	309.35			313.05		
0.240	308.65			312.55		
0.276		308.15			312.48	
0.287		308.10			312.47	
0.300		308.00			312.45	
0.342		307.45			312.40	
0.425		306.35			312.33	
0.475		305.90			312.10	
0.500		305.30			312.25	
0.512		305.30			311.98	
0.535		304.92			312.15	
0.540		304.85			312.15	
0.600			304.15			312.20
0.644			303.95			311.90
0.765			303.85			312.15

This pretransition, omitted on the thermogram given in Figure 1, represents a phase change from the $L_{\beta'}$ lamellar gel to the $P_{\beta'}$ rippled gel phase,[24,25,29] and is attributed primarily to the reorientation of the DPPC bilayer surfaces.[21,22] The DPPC pretransition is diminished to nondetectable levels at the lowest mole fraction of UDCA employed (X_{UDCA} around 0.054), an effect of UDCA perhaps originating from specific interfacial interactions between the polar groups of UDCA molecule and the DPPC headgroups in which hydration shells surrounding the zwitterionic headgroups are perturbed. Similar effects on the pretransition of DPPC bilayers have been reported for the action of various amphiphillic molecules, such as halothane[37] or the palmitoyl derivative of alpha-bungarotoxin,[23] for comparable ranges of concentrations.

As shown in Figures 1 and 2, the interaction of UDCA with DPPC bilayers induces a broadening and decrease in height in the main endotherm. This effect may arise from several sources, for example, from the presence of various sizes of DPPC L_α

TABLE 3: Thermotropic Phase Transition Enthalpies Exhibited by DPPC and UDCA at pH 7

sample	transition enthalpy (ΔH) (kcal/mole)		
X_{UDCA}	gel/L_α	L_{gI}/L_α	$L_{g'}/L_\alpha$
0.000	8.50 ± 0.10		
0.054	8.54 ± 0.12		
0.065	8.65 ± 0.11		
0.085	8.52 ± 0.15		
0.125	8.60 ± 0.10		
0.150	8.65 ± 0.11		
0.175	8.50 ± 0.12		
0.210	8.49 ± 0.14		
0.240	8.51 ± 0.14		
0.276		8.60 ± 0.12	
0.287		8.65 ± 0.12	
0.300		8.80 ± 0.15	
0.342		8.75 ± 0.16	
0.400		8.90 ± 0.15	
0.425		9.15 ± 0.14	
0.475		9.30 ± 0.12	
0.500		9.40 ± 0.14	
0.535		9.78 ± 0.20	
0.540		9.70 ± 0.20	
0.600			9.75 ± 0.18
0.644			9.83 ± 0.20
0.765			9.84 ± 0.19

(liquid crystalline) clusters in equilibrium with the gel clusters that define the phase transition, from the heterogeneity of various molecular DPPC:UDCA aggregates or interfacial associations, and from the formation of bilayer microdomains. The large widths observed for the main DPPC phase transition, given by the temperature spans in Table 2 and displayed in Figure 3B, indicate that nearly all UDCA molecules are either adsorbed or are incorporated into DPPC bilayers, with the number of free UDCA in the aqueous phase being nearly depleted. This behavior is similar to that of lipid bilayers in the presence of anesthetics.[38]

III. Phase Diagram. Plots of the main transition temperatures (T_m) of DPPC bilayers as a function of increasing UDCA concentration display three separate regions, as shown in Figure 3A and summarized in Table 1. In region 1, encompassing mole fractions $X_{UDCA} < 0.25$, T_m decreases linearly and more steeply than the T_m's for region 2 (for $0.25 < X_{UDCA} < 0.60$). For region 1, extrapolation of the line to zero UDCA concentration gives an intercept of 314.47 ± 0.06 K, a value close to T_m° = 314.50 ± 0.05 K measured for pure DPPC bilayers (Figure 1 and Table 1). This observation suggests that up to a critical concentration of 25 mol % of UDCA (corresponding to a UDCA:DPPC mole ratio of 1:3), DPPC molecules remain arranged in a bilayer structure in the mixed gel (L_g) state similar to the conventional $L_{\beta'}$ gel phase of pure DPPC bilayers. This lamellar L_g structure, facilitated by the predominant interfacial interactions between the bilayer and bile salt, is supported by experimental data indicating that the DPPC $L_{\beta'}$ to $P_{\beta'}$ phase pretransition vanishes in the presence of UDCA. This suggested L_g structure is analogous to those reported for related bile salt/lecithin systems rich in lecithin, which have been studied by calorimetric[4] and X-ray small-angle scattering methods.[5] Thus, the phase transitions recorded for mixed DPPC:UDCA dispersions (X_{UDCA} increasing to about 0.25) are consistent with bilayer transitions from the L_g phase to the L_α phase, but with the transition temperatures linearly depressed.

The first change in slope for the T_m versus X_{UDCA} plots occurs for X_{UDCA} of about 0.25 (Figure 3A) and suggests that the structure of the mixed DPPC:UDCA dispersions is fundamentally altered at a mole ratio for DPPC:UDCA of 3:1; that is, a new mixed gel phase, denoted L_{gI}, is formed. As the UDCA concentration increases ($X_{UDCA} > 0.25$, corresponding to region 2 in Figure 3A), a second change in slope occurs at a critical concentration of X_{UDCA} at around 0.60. This is the apparent concentration limit of the formation of this new induced phase, L_{gI}, a phase analogous, for example, to that reported for DPPC bilayers in the presence of various surface active species.[26−30] We will identify the L_{gI} phase with an interdigitated chain morphology. Supporting this identification are the Raman spectroscopic order/disorder parameters for the acyl chains of DPPC bilayers in aqueous dispersions in the presence of UDCA which are consistent with the development of an interdigitated or partially interdigitated DPPC gel (L_{gI}) phase (unpublished data).[31a] Briefly, the Raman spectroscopic lateral interchain order/disorder parameters are monitored by the $I(2850\ cm^{-1})/I(2880\ cm^{-1})$ peak height intensity ratios of the symmetric and asymmetric methylene C−H stretching modes, respectively. For pure gel phase DPPC multilayers the value for this index is typically 0.77 ± 0.02, which is characteristic of a bilayer system whose chains are hexagonally packed. Comparisons of this intensity ratio with systems known from X-ray diffraction studies to be interdigitated exibit lower values of this index in the $I(2850\ cm^{-1})/I(2880\ cm^{-1})$ range of 0.65−0.70.[31b] Our unpublished Raman data for UDCA yield values of 0.68 ± 0.02 for the lateral chain−chain index, values suggestive of an interdigitated chain membrane morphology. The L_{gI} structure is in accord with partition equilibria and changes in melting enthalpies (vide infra).

At approximately 60 mol % UDCA, corresponding to a mole ratio DPPC:UDCA of 2:3, a third region of the phase diagram emerges (region 3, Figure 3A). In this concentration interval T_m values seem to remain approximately constant at 309.15 ±

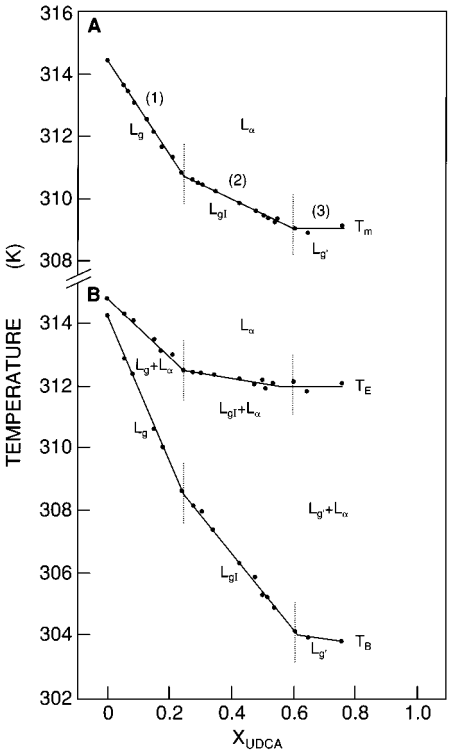

Figure 3. Phase diagram of DPPC:UDCA dispersions. (A) Temperature of main transition, T_m, of DPPC dispersions containing various amounts of UDCA (given in Table 1). The line of region 1 and of region 2 is a least-squares linear regression with a slope of $(dT_m/dX_{UDCA})_1 = -15.153 \mp 0.171$ and of $(dT_m/dX_{UDCA})_2 = -5.222 \mp 0.018$, respectively, expressed in °C/unit mole fraction and an intercept of 314.47 ± 0.06 K and of 312.12 ± 0.11 K, respectively, with a correlation coefficient $r_1 = -0.9987$ and $r_2 = -0.9975$, respectively. (B) Plots of the onset (T_B) and completion (T_E) temperatures of endothermic phase transition (given in Table 2).

0.25 K. Presumably, either once UDCA molecules are incorporated into the DPPC bilayers, a constant stoichiometric relation between UDCA and DPPC occurs or the L_{gI} gel coexists in equilibrium with micelles of various UDCA:DPPC mole ratios. The structure of this phase, which we term the mixed "micellar" gel (noted $L_{g'}$), remains to be elucidated. Region 3 of the phase diagram appears to be consistent with a transition from mixed micellar $L_{g'}$ gel to the liquid crystalline L_α phase. A mixed micelle model for this system is supported also by a wide variety of experimental techniques[1−16] applied to related systems containing lecithins and bile acids or bile salts in similar concentration ranges.

The endotherm peaks in the thermograms shown in Figures 1 and 2 can be further characterized by a plot of the onset (T_B) and completion (T_E) temperatures, as delineated in Figure 3B. The T_B and T_E temperatures were determined by taking the base line intercepts of the relatively sharp features of endotherms at the low and high-temperature extremes, respectively.[39] The T_B and T_E values are also given in Table 2 as a function X_{UDCA}. The upper T_E and lower T_B temperatures define liquidus and solidus curves, respectively (Figure 3B). The liquidus curve delineates the boundary between the liquid crystalline, single-phase (high temperature, L_α phase) and lower temperature region (two-phase region containing the liquid crystalline and a given gel phase). The solidus curve represents the boundary between the low-temperature gel single-phases, L_g, L_{gI}, or $L_{g'}$, and the two-phase region. The characteristic feature of Figure 3B is that the liquidus and solidus lines diverge with the increasing UDCA concentrations and show changes in slope at mole fractions X_{UDCA} of about 0.25 and 0.60. These data agree with the data plotted in Figure 3A for the DPPC:UDCA mole ratios of 3:1 and 2:3 and indicate that new structural mixed phases are formed for these critical concentrations.

IV. Thermodynamic Analysis of UDCA Partition Equilibria. A thermodynamic analysis of the decrease in melting temperatures T_m of DPPC bilayers, as a function of UDCA, leads to an estimate of the bilayer composition. Considering ideal solution theory and that UDCA is miscible with DPPC only in the liquid crystalline L_α phase, we express the Schroder and van Laar's relation[40] as

$$\ln X_{DPPC}{}^{b} = -(\Delta H°/R)\,(1/T_m - 1/T_m°) \qquad (1)$$

where $X_{DPPC}{}^{b}$ is the mole fraction of DPPC in bilayers. $\Delta H°$ equals $\Delta H°_{DPPC}$ and represents the main phase transition enthalpy of pure DPPC bilayers at temperature $T_m°$, which is assumed to be temperature independent. $T_m°$ and T_m are the main transition temperatures for the pure DPPC bilayers and mixed DPPC:UDCA bilayers, respectively. R is the gas constant.

The quantity $X_{UDCA}{}^{b}$ represents the mole fraction of UDCA incorporated into the DPPC bilayer with $X_{DPPC}{}^{b} + X_{UDCA}{}^{b} = 1$. For a dilute bilayer mixture,[40] $\ln(1 - X_{UDCA}{}^{b}) = -X_{UDCA}{}^{b}$. Rearranging and simplifying eq 1, we obtain

$$\Delta T_m = R(T_m°)^2\, X_{UDCA}{}^{b}/\Delta H° \qquad (2)$$

where

$$\Delta T_m = T_m° - T_m \qquad (3)$$

defines the melting temperature depression of the DPPC bilayers. (Frequently, the approximation $T_m°T_m = (T_m°)^2$ is used.[38,40−42] Thus, eq describes the shape of melting curves given in Figure 3A. The partition coefficient of UDCA between the DPPC bilayers and bulk aqueous solution K_b is defined by

$$K_b = X_{UDCA}{}^{b}/X_{UDCA}{}^{w} \qquad (4)$$

where $X_{UDCA}w$ is the mole fraction of UDCA in aqueous solution, noted as phase w. Equations 2 and 4 yield

$$\Delta T_m = R(T_m°)^2 K_b X_{UDCA}{}^{w}/\Delta H° \qquad (5)$$

where the quantity $R(T_m°)^2/\Delta H°$, or A_o, is approximately equal to 23 K, using experimental values for pure DPPC bilayers of $\Delta H° = 8.5$ kcal/mol and $T_m° = 314.5$ K. By assuming a direct dependence of $X_{UDCA}{}^{w}$ with X_{UDCA} (total mole fraction of UDCA in that system), eq 5 is expressed as

$$\Delta T_m = A_o K_{b,app} X_{UDCA}$$

where $K_{b,app}$ represents the apparent partition coefficient of UDCA between DPPC (L_α) bilayers and the aqueous buffer phase. This model, a limiting case, assumes that UDCA molecules are excluded from the DPPC gel phase. More likely, however, the UDCA binding or partitioning to DPPC gel structures is not negligible. The important point to note is that the various slope changes in the phase diagram shown in Figure 3A indicate changes in UDCA partition coefficients in agreement with eq 5 and suggest that structural transformations are induced in DPPC bilayers at corresponding critical UDCA concentrations.

Analogous relations for changes in the transition temperatures can be proposed using the equilibria equations:

$$UDCA_w \overset{K_{L\alpha}}{\leftrightarrow} UDCA_{L\alpha} \overset{K}{\leftrightarrow} UDCA_g \qquad (6)$$

which combine the partitioning of UDCA between DPPC liquid crystalline L_α bilayers and the aqueous phase (reflecting a partition coefficient $K_{L\alpha}$) with a partitioning of UDCA between the DPPC gel (g) phase and DPPC L_α structures (characterized by a partition coefficient K). Therefore, in considering the equilibria in eq 6, eq 5 becomes

$$\Delta T_m = R(T_m°)^2(1 - K)K_{L\alpha}\, X_{UDCA}{}^{w}/\Delta H° \qquad (7)$$

where $K_{L\alpha}$ and K are defined by

$$K_{L\alpha} = X_{UDCA}{}^{L\alpha}/X_{UDCA}{}^{w} \quad \text{and}$$

$$K = X_{UDCA}{}^{g}/X_{UDCA}{}^{L\alpha}, \text{ respectively}$$

Equation 7 demonstrates that the shift of the main phase transition ΔT_m is decreased by UDCA partitioning between bilayer phases, represented by the partition coefficient K, where K is characteristic of the bilayer states in equilibrium. Furthermore, by examining the partitioning behavior of UDCA between the DPPC gel phase and buffer (characterized by K_g) and between the DPPC L_α phase and buffer (given by $K_{L\alpha}$), we extend the above equations through similar procedures using the following equilibria conditions:

$$\begin{array}{ccc} UDCA_w & \overset{K_{L\alpha}}{\Longleftrightarrow} & UDCA_{L\alpha} \\ {\scriptstyle K_g}\,\diagdown\!\diagdown & & \diagup\!\diagup\,{\scriptstyle K} \\ & UDCA_g & \end{array} \qquad (8)$$

These relationships assume the miscibility of DPPC with UDCA in both bilayer structures (g and L_α). Equation 1 then becomes

$$\ln X_{\mathrm{DPPC}}{}^{\mathrm{g}}/X_{\mathrm{DPPC}}{}^{\mathrm{L}\alpha} = \Delta H^{\circ}R^{-1}(1/T_{\mathrm{m}} - 1/T_{\mathrm{m}}{}^{\circ}) = \ln[(1 - X_{\mathrm{UDCA}}{}^{\mathrm{g}})/(1 - X_{\mathrm{UDCA}}{}^{\mathrm{L}\alpha})] \quad (9)$$

where $X_{\mathrm{DPPC}}{}^{\Phi}$ and $X_{\mathrm{UDCA}}{}^{\Phi}$ represent the molar fraction of DPPC and UDCA, respectively, in phase Φ, i.e., the g and/or the L_α bilayer phases. Rearrangment and simplification of eq 9 yield

$$\Delta T_{\mathrm{m}} = R(T_{\mathrm{m}}{}^{\circ})^2(K_{\mathrm{L}\alpha} - K_{\mathrm{g}})X_{\mathrm{UDCA}}{}^{\mathrm{w}}/\Delta H^{\circ} \quad (10)$$

where by definition,

$$K_{\mathrm{g}} = X_{\mathrm{UDCA}}{}^{\mathrm{g}}/X_{\mathrm{UDCA}}{}^{\mathrm{w}}$$

A comparison between equations 10 and 7 relates K, the UDCA partition coefficient between the gel and liquid crystalline phases, to $K_{\mathrm{L}\alpha}$ and K_{g} by

$$K = K_{\mathrm{g}}/K_{\mathrm{L}\alpha} \quad (11)$$

Alternatively, eq 10 can be written as:

$$\Delta T_{\mathrm{m}} = A_{\mathrm{o}}\, K_{\mathrm{app}}\, X_{\mathrm{UDCA}} \quad (12)$$

where K_{app} is an apparent total partition coefficient of UDCA between various phases in equilibrium in mixed systems.

Thus, the above eqs 7, 10, or 12 predict both the linear decrease of ΔT_{m} with the increasing UDCA concentration and the changes in slopes as a function of a putative change in the structure of the DPPC bilayer. On the basis of this treatment, the UDCA partition into the L_{gI} gel phase, which we suggest may be an interdigitated acyl chain structure, is greater than in the conventional noninterdigitated lamellar (L_{g}) gel phase.

The phase diagram shown in Figure 3 is also consistent with a model stating that, as more UDCA molecules are partitioned through either adsorption or incorporation into the DPPC interdigitated L_{gI} phase, in comparison to the L_{g} phase, then the partitioning into a mixed micellar gel phase $L_{\mathrm{g}'}$ becomes comparable with that for the L_α phase, especially at high UDCA concentrations. This is reasonable, since the DPPC hydrocarbon chains in the putative interdigitated L_{gI} gel phase would increase the total surface area of bilayers in contrast to conventional lamellar (L_{g}) gel. Similarly, since the total surface area of the mixed $L_{\mathrm{g}'}$ micellar gel is greater than that in the L_{gI} gel phase, it follows that more binding sites for UDCA in the L_{gI} and $L_{\mathrm{g}'}$ phases are available than in the L_{g} phase.

V. Transition Enthalpies. For the equilibrium gel (g) to liquid crystalline (L_α) phase transition, the transition enthalpy ΔH, corresponding to the heat of melting of the gel phase for a DPPC:UDCA mixture at $T = T_{\mathrm{m}}$, under constant external pressure, is defined by

$$\Delta H(T_{\mathrm{m}},n_{\mathrm{DPPC}},n_{\mathrm{UDCA}}) = H_{\mathrm{L}\alpha}(T_{\mathrm{m}},n_{\mathrm{DPPC}},n_{\mathrm{UDCA}}) - H_{\mathrm{g}}(T_{\mathrm{m}},n_{\mathrm{DPPC}},n_{\mathrm{UDCA}}) \quad (13)$$

where H_Φ is the enthalpy of phase Φ, and n_{i} is the number of moles of component i in the system. Similarly, the molar transition enthalpy for pure DPPC bilayers, occurring at temperature $T_{\mathrm{m}}{}^{\circ}$, is given as

$$\Delta H^{\circ}{}_{\mathrm{DPPC}}(T_{\mathrm{m}}{}^{\circ}) = H_{\mathrm{L}\alpha}(T_{\mathrm{m}}{}^{\circ}) - H_{\mathrm{g}}(T_{\mathrm{m}}{}^{\circ}) \quad (14)$$

where the (g) phase reflects the $P_{\beta'}$ rippled gel phase for pure DPPC bilayers. The molar transition enthalpies of DPPC bilayers both in the absence ($\Delta H^{\circ}{}_{\mathrm{DPPC}}$) and in the presence of UDCA (ΔH) were determined by the integration of the DSC curves, which are plotted in terms of excess molar heat capacity as a function of temperature.[43] Furthermore, we emphasize that the net calorimetric enthalpies are determined by the differences in physical and chemical properties between the liquid crystalline and gel phases and not solely by the properties of one specific phase.

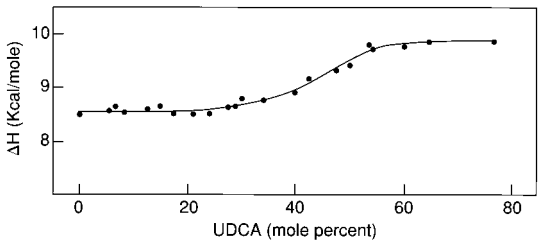

Figure 4. The molar transition enthalpy ΔH (kcal/mole, in Table 3) of DPPC bilayers, with DPPC concentrations of approximately 10 mM, given as a function of UDCA concentration (expressed in mole %) in mixed DPPC:UDCA dispersions. See Figure 3 for other conditions.

The enthalpy determinations for the UDCA:DPPC bilayers are illustrated in Figure 4 and presented in Table 3 as a function of UDCA composition expressed in mole % and X_{UDCA}, respectively. For the mixed DPPC:UDCA bilayers in the range for $0 < X_{\mathrm{UDCA}} < 0.25$, the main mixed gel ($L_{\mathrm{g}}$) to mixed L_α phase transition is reflected by a constant molar melting enthalpy of 8.55 ± 0.15 kcal/mol, which is equivalent to $\Delta H^{\circ}{}_{\mathrm{DPPC}}$. That is, the UDCA induced alterations in both the molecular packing characteristics and the acyl chain dynamics of the perturbed DPPC bilayers are compensated appropriately in either the conventional bilayer L_{g} gel phase structure or the L_α phase of the mixed DPPC:UDCA bilayers.

As shown in Figure 4, ΔH increases at compositions for which a new L_{gI} mixed gel is induced for the concentration range $0.25 < X_{\mathrm{UDCA}} < 0.60$, in agreement with the phase diagram in Figure 3. This increase in ΔH persists to around 75 mol % UDCA in the DPPC dispersions, the point at which the L_{gI} phase probably coexists with micelles. A conversion of DPPC molecules to specific complexes with UDCA for mole ratios of UDCA:DPPC from 3:2 or 3:1 can be assumed. These molecular complexes may be responsible, in part, for the observed broad transitions and temperature span of the phase diagram. The structure of this mixed or "micellar" $L_{\mathrm{g}'}$ gel phase for $X_{\mathrm{UDCA}} > 0.60$, remains to be elucidated.

We have associated the new gel structure, induced at intermediate UDCA concentrations in DPPC dispersions, with an interdigitated (L_{gI}), mixed DPPC:UDCA gel phase. Since related interdigitated chain systems [27,28,30] indicate that the van der Waals' interactions between chains are greater in the L_{gI} phase than in a conventional, noninterdigitated L_{g} gel phase, the observed increase in melting enthalpies (Figure 4) for the assigned L_{gI} phase is consistent with some degree of bilayer acyl chain interdigitation being induced by UDCA interactions. These data also suggest that the primary effect of UDCA molecules in inducing chain interdigitation occurs at the interfacial region of the bilayer, a location where UDCA would replace water molecules presumably by lying parallel to the bilayer surface. This configuration would balance the unfavorable exposure of the terminal acyl chain methyl groups of DPPC to interfacial water. Thus, the differences in observed thermodynamic quantities reflect both interfacial energetics and ordering properties of the bilayer core in the different structures spanning the lamellar, noninterdigitated gel (L_{g}, e.g., mixed DPPC dispersions, rich in phospholipid), the interdigitated gel (L_{gI}, at intermediate UDCA concentrations) to the mixed "micellar" gel ($L_{\mathrm{g}'}$, e.g. DPPC dispersions, rich in UDCA) phases.

VI. UDCA:DPPC Molecular Interactions. Figures 1 and 2 indicate that the DPPC phase transition is strongly affected by the presence of UDCA, behavior analogous to the effects of various amphiphilic compounds.[23,24,44] The behavior of the DSC thermograms can be understood by assuming that the bilayer perturbations from UDCA involve the superposition of several intermolecular effects including interfacial, hydrogen bonds and nonspecific hydrophobic and electrostatic interactions. These result in composition-driven changes in the DPPC bilayer organization which are reflected by Figure 3. In mixed DPPC:UDCA bilayers, we expect a substantial fraction of UDCA molecules to lie with their fused ring systems in a parallel orientation on the DPPC bilayer surface as a result of the hydrophilic−hydrophobic nature[16,45] of the two UDCA molecular sides, as was concluded for lipid bilayer systems containing either cholate,[6] or taurocholate[12] or taurodeoxycholate.[13,14] Since the adsorbed UDCA molecules influence the average interfacial orientation of the DPPC bilayer headgroups, a propagation of these interfacial energetics should influence the lipid-packing properties within the DPPC bilayer core. As shown in Figure 3, a break point in the gel to liquid crystalline phase transition temperatures occurs for a UDCA:DPPC mole ratio of about 1:3. Analogous to other systems, we suggest that a mixed interdigitated gel phase is induced at these concentrations. Concomitantly, UDCA exerts a stabilizing effect on DPPC bilayers, which is observed for UDCA concentrations greater than 25 mol % and reflected by increased values in the transition enthalpies.

Statistically, a population of UDCA molecules could be accommodated between the DPPC acyl chains through nonspecific hydrophobic interaction, as observed for steroids intercalated within endoplasmic reticulum membranes.[46] Whether UDCA interacts either peripherally or intrinsically with the DPPC bilayers, the packing arrangements of the DPPC hydrocarbon chains would be perturbed, which, in turn, would alter the order−disorder transitions of mixed component bilayer dispersions. Additionally, defects probably arising at the boundaries between microdomains formed within UDCA:DPPC bilayers could provide loci for increased UDCA adsorption and/or penetration into the bilayer. Since the adsorption of UDCA molecules by the DPPC bilayers would modulate and ultimately decrease the edge tension of the bilayer by integrating UDCA,[47] the fragmentation of these mixed systems would be expected. As a consequence, a fragmented interdigitated gel phase may coexist in equilibrium with micelles of different UDCA:DPPC internal compositions, particularly for DPPC:UDCA systems highly rich in UDCA. Such a resulting mixed "micellar" gel phase, supported by literature evidence on related assemblies,[4−6] remains to be structurally investigated.

VII. Gibbs Free Energies. Figure 5 displays the bilayer Gibbs free energy G of the gel and the liquid crystalline phases of DPPC, as a function of temperature, in the presence of various UDCA perturbations. The changes in the associated bilayer Gibbs free energies (ΔG) at the transition temperature are also presented in Figure 5; free energy changes for pure DPPC bilayers are shown in part A, while parts B and C present the data for the mixed DPPC:UDCA assemblies. The bilayer Gibbs free energy G_Φ, where the subscript Φ delineates a phase classification, is given by $G_\Phi = H_\Phi - TS_\Phi$, where $G_\Phi = G_\Phi(T,p,n_i\Phi)$; p is the external pressure and $n_i\Phi$ is the number of moles of component i in phase Φ. For the purpose of clarity, both the enthalpy H_Φ and entropy S_Φ are assumed to be constant; that is, they are independent of temperature in the range for each phase Φ.

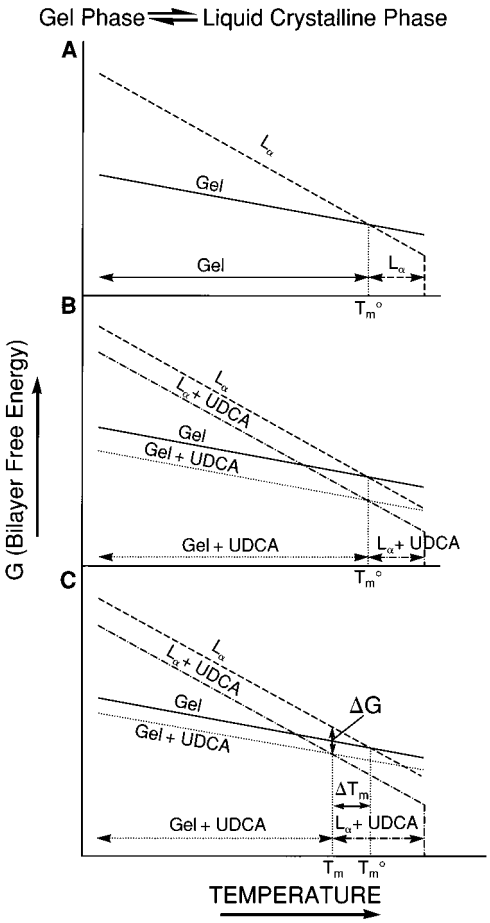

Figure 5. Schematic diagrams of the bilayer Gibbs free energy, G, as a function of temperature, T increasing from left to the right. Part A represents G for the gel (solid line) and of liquid crystalline (dashed line) DPPC bilayers in the absence of UDCA. Part B shows the perturbation of UDCA partitioned equally into mixed gel (gel+UDCA) and mixed liquid crystalline (L_α+UDCA) phases. Part C describes the perturbations of UDCA, reduced by a factor of 2, in the mixed DPPC:UDCA gel phase in comparison to the mixed liquid crystalline phase. The dotted lines indicate the Gibbs free energy of the mixed gel phase in the presence of various UDCA concentrations (B and C), while the dot−dashed line represents the effects of UDCA in lowering the Gibbs free energy of the mixed liquid crystalline phase. Horizontal arrows represent the ranges of temperature over which each of the two phases exist. See the text for the definitions of the symbols.

The rippled $P_{\beta'}$ gel to liquid crystalline L_α phase transition occurs at a temperature $T_m°$, as shown in Figure 5A. At this temperature the L_α phase (thermodynamically favored above $T_m°$) and the $P_{\beta'}$ phase (or g phase, with the lowest free energy below $T_m°$) have identical free energies, ($\Delta G(T_m°) = 0$) and $G_{L\alpha}(T_m°) = G_{P\beta'}(T_m°)$. Furthermore, we assume that the effects of UDCA decrease the bilayer Gibbs free energy. This assumption permits us to represent the free energy of the mixed gel phase, denoted as gel+UDCA or g, and of the mixed liquid crystalline phase, L_α+UDCA, below and parallel to the free energy of the pure DPPC bilayer. When the UDCA perturbations are equal in both the gel and the liquid crystalline DPPC phases, the gel to liquid crystalline transition occurs at $T_m = T_m°$ (Figure 5B). In particular, if it is assumed that K = 1, or $K_{L\alpha} = K_g$, the UDCA concentration in the mixed fluid L_α phase becomes equal to the concentration in the mixed gel phase of the DPPC:UDCA bilayer. Under these conditions eq 7 and eq 10 give independently $\Delta T_m = 0$. Therefore, on the basis of the partition equilibrium, the gel to liquid crystalline transition temperature also occurs at $T_m = T_m°$. In addition, the differential partitioning of UDCA between the various DPPC bilayer

structures modulates the equilibrium between those phases. For example, as shown in Figure 5C, if the perturbations of UDCA are reduced 2-fold in the mixed gel DPPC structure compared to the mixed liquid crystalline phase, then the DPPC melting transition temperature is depressed; that is, $T_m < T_m°$. The relationship between ΔT_m and the partition coefficient of UDCA either within the bilayer structure, denoted by K, or between the various bilayer states and the aqueous solution, denoted by K_g and $K_{L\alpha}$, and given by eqs 7 and 10, respectively, also explain the above depression in transition temperature. For example, under the condition of $K < 1$, eq 1 shows that $K_{L\alpha} > K_g$ and, as a consequence, a greater quantity of UDCA will be distributed in the mixed L_α phase in comparison to the mixed gel phase. In this instance, eqs 7 and 10 predict a depression of $T_m°$ in a similar fashion, as illustrated in Figure 5C.

We can derive from eqs 7 and 10 several general rules concerning the UDCA partition equilibria either within the DPPC bilayer structures or between the bilayers and the aqueous phase. For example, the UDCA partition coefficients decrease in the following order: $K_{L\alpha} > (K_g)L_{gI} > (K_g)L_g$, which explains regions 1 and 2 in Figure 3A. Furthermore, since the partition of UDCA in the mixed "micellar" gel ($L_{g'}$) phase is comparable with that in the mixed liquid crystalline phase, $K_{Lg'} = K_{L\alpha}$. This behavior is supported by region 3, obtained experimentally, and is given in Figure 3A. Therefore, the UDCA solubility, expressed in terms of its adsorption and incorporation into the DPPC bilayers, increases in the order $L_g < L_{gI} < L_{g'} = L_\alpha$.

To provide a description of the electrostatic contributions to the interaction energetics of UDCA and DPPC bilayers, we employ a perturbation approach.[24,48−51] In the perturbation model,[48−51] the total free energy change $\Delta G(T_m)$ associated with the incorporation of UDCA into the DPPC bilayers can be written as the sum of the following free energies: $\Delta G(T_m) = \Delta G_{pl} + \Delta G_h + \Delta G_{el} + \Delta G_{hb} + \Delta G_w$, which involve acyl chain interdigitation (ΔG_{pl}), hydration (ΔG_h), electrostatic interactions (ΔG_{el}), hydrogen bonding (ΔG_{hb}), and hydrophobic interactions (ΔG_w). As an example, the contribution of anionic $UDCA^-$ molecules binding to the zwitterionic phosphatidylcholine bilayers can be given by the change in the electrostatic bilayer free energy (ΔG_{el}) at the phase transition.[48,49] From this, ΔG_{el} becomes proportional to the electrostatic bilayer lateral pressure π_{el}; that is, $\Delta G_{el} = \pi_{el}\Delta A$, where ΔA is the change in the lipid area at the phase transition. Experimentally, this contribution could be quantitated by Langmuir−Blodgett film techniques. Thus, the bilayer surface charge created by the adsorption and/or incorporation of UDCA into DPPC bilayers contributes to the decrease of the chain-melting transition temperature, in a similar way as found on related systems.[24] The primary argument is that the electrostatically induced transition temperature shifts increase linearly with increasing the surface charge density,[50] which explains, in part, the linear decrease in T_m with increasing UDCA concentrations (region 1, in Figure 3A). Furthermore, at $X_{UDCA} = 0.25$, another dominant effect occurs; namely, that the suggested interdigitation of the acyl chains within the DPPC bilayers decreases the slope of the linear dependence of ΔT_m with X_{UDCA} (see region 2 in Figure 3A) and increases the melting transition enthalpy of DPPC from the L_{gI} to the L_α phase (Figure 4).

Conclusions

We have developed a thermodynamic approach for elucidating the phase transitions within aqueous DPPC bilayer dispersions in the presence of UDCA. This approach allows us to interpret partition equilibria of UDCA between various DPPC bilayer structures and between bilayers and the aqueous solution. Specifically, expressions are derived for describing the main transition temperatures (T_m) of mixed DPPC:UDCA dispersions as functions of the partition equilibria of UDCA. These expressions, together with the transition data, enthalpies, and Gibbs free energies, are used to construct the phase diagrams, to interpret the DPPC phase structural changes, and to estimate the specific UDCA concentration ranges determining a given mixed phase.

In particular, at mole fractions of UDCA smaller than 0.25, the mixed DPPC:UDCA conventional lamellar (noninterdigitated) gel persists. At mole fractions of UDCA greater than 0.25, the putative interdigitated L_{gI} bilayer gel of DPPC and UDCA is induced. The transition enthalpies reflect an increased interaction within the L_{gI} phase and are consistent with the phase diagram and UDCA partition coefficients between the various DPPC bilayer structures. At mole fractions of UDCA greater than 0.60, a new thermal phase forms that could consist of an interdigitated gel in equilibrium with the mixed UDCA:DPPC micelles of various internal compositions. This mixed "micellar" gel yields thermal transitions close to 309.15 K.

This study of the effects of ursodeoxycholic acid and ursodeoxycholate on aqueous dipalmitoyl phosphatidylcholine bilayer dispersions at pH 7.0 clearly indicates that several different membrane perturbations are induced by these surfactants. Similar effects may appear in phospholipid bilayers of biological membranes (e.g., hepatocyte membranes) under certain conditions and may critically depend both on membrane lipid composition and, particularly, on the presence of amphiphilic compounds, such as the more hydrophilic bile acids and their bile salts. Further detailed knowledge of the mechanisms by which ursodeoxycholic acid and its salt perturb both model and cellular membranes should substantially contribute to our understanding of many of the complex processes associated with membrane phenomena and perhaps lead ultimately to model compounds designed for eliciting specific membrane effects.

Acknowledgment. M. Tomoaia-Cotisel acknowledges financial support from the National Institute of Arthritis and Musculoskeletal and Skin Diseases during the course of this work. The authors also acknowledge helpful discussions with Dr. E. N. Lewis, Dr. S. Tomellini, Dr. J. T. Mason, and Dr. R. G. Adams.

Glossary

K_b:	the partition coefficient of UDCA between the DPPC bilayers and buffer
K:	the partition coefficient of UDCA between DPPC gel and DPPC liquid crystalline phase
$K_{L\alpha}$:	the partition coefficient of UDCA between DPPC liquid crystalline bilayers and buffer
K_g:	the partition coefficient of UDCA between the DPPC gel phase and buffer
$T_p°$:	pretransition temperature of pure DPPC bilayers, from $L_{\beta'}$ to $P_{\beta'}$ phase
$T_m°$:	main transition temperature of pure DPPC bilayers, from $P_{\beta'}$ to L_α phase
T_m:	melting temperature of mixed (DPPC:UDCA) dispersions
$T_{onset} = T_B$:	onset temperature of endothermic transitions
$T_{completion} = T_E$:	completion temperature of endothermic transitions
H_Φ:	the enthalpy of Φ phase
$\Delta H°_{p,DPPC}$:	the molar pretransition enthalpy of pure DPPC bilayers
$\Delta H°_{DPPC}$:	the molar (gel to liquid crystalline phase) transition enthalpy of pure DPPC bilayers

ΔH:	the molar (gel to liquid crystalline phase) transition enthalpy of mixed DPPC:UDCA dispersions
$X_i\Phi$	the mole fraction of component i in phase Φ
$n_i\Phi$	the number of moles of component i in phase Φ
X_{DPPC}	the total mole fraction of DPPC in aqueous dispersions
X_{UDCA}	the total mole fraction of UDCAH and $UDCA^-$ in aqueous dispersions
G_Φ	Gibbs free energy of Φ phase
L_α	liquid crystalline phase
g	gel phase
$L_{\beta'}$	lamellar gel phase
$P_{\beta'}$	rippled gel phase
L_g	lamellar noninterdigitated mixed (DPPC:UDCA) gel phase
L_{gI}	interdigitated mixed gel phase
$L_{g'}$	mixed "micellar" gel phase

Abbreviations

DSC	differential scanning calorimetry
DPPC	1,2-dipalmitoyl-*sn*-glycero-3-phosphocholine or dipalmitoyl phosphatidylcholine
UDCAH:	ursodeoxycholic acid: 3α,7β-dihydroxy-5β-cholan-24-oic acid
$UDCA^-$	ursodeoxycholate
UDCA	total concentration of all (UDCAH and $UDCA^-$) molecular species

References and Notes

(1) Small, D. M.; Bourges, M. C.; Dervichian, D. G. *Biochim. Biophys. Acta* **1966**, *125*, 563−580.
(2) Small, D. M. In *The Bile Acids*; Nair, P. P., Kritchevsky, D., Eds.; Plenum: New York, 1971; Vol. 1, pp 249−356.
(3) Mazer, N. A.; Benedek, G. B.; Carey, M. C. *Biochemistry* **1980**, *19*, 601−615.
(4) Claffey, W. J.; Holzbach, R. T. *Biochemistry* **1981**, *20*, 415−418.
(5) Muller, K. *Biochemistry* **1981**, *20*, 404−414.
(6) Ulmius, J; Lindblom, G; Wennerstrom, H.; Johansson, L. B.-A.; Fontell, K.; Soderman, O; Arvidson, G. *Biochemistry* **1982**, *21*, 1553−1560.
(7) Schurtenberger, P.; Mazer, N.; Kanzig, W. *J. Phys. Chem*. **1985**, *89*, 1042−1049.
(8) Montet, J.-C. *Pathol. Biol*. **1991**, *39*, 621−624.
(9) Malloy, R. C.; Binford, J. S., Jr. *J. Phys. Chem*. **1990**, *94*, 337−345.
(10) Nagata, M.; Yotsuyanagi, T.; Ikeda, K. *Chem. Pharm. Bull*. **1990**, *38*, 1341−1344.
(11) Spink, C. H.; Lieto, V.; Mereand, E.; Pruden, C. *Biochemistry* **1991**, *30*, 5104−5112.
(12) Hjelm, R. P., Jr.; Thiyagarajan, P.; Alkan-Onyuksel, H. *J. Phys. Chem*. **1992**, *96*, 8653−8661.
(13) Long, M. A.; Kaler, E. W.; Lee, S. P.; Wignall, G. D. *J. Phys. Chem*. **1994**, *98*, 4402−4410.
(14) Long, M. A.; Kaler, E. W.; Lee, S. P. *Biophys. J*. **1994**, *67*, 1733−1742.
(15) Egelhaaf, S. U.; Schurtenberger, P. *J. Phys. Chem*. **1994**, *98*, 8560−8573.
(16) Jones, M. N.; Chapman, D. *Micelles, Monolayers, and Biomembranes*; Wiley-Liss: New York, 1995; Chapters 1 and 3.
(17) Carey, M. C.; Montet, J.-C.; Phillips, M. C.; Armstrong, M. J.; Mazer, N. A. *Biochemistry* **1981**, *20*, 3637−3648.
(18) Hofmann, A. F. Scand. J. *Gastroenterol.* **1994**, 29 (Suppl. 204), 1−15.
(19) Paumgartner, G.; Pauletzki, J.; Sackmann, M. *Scand. J. Gastroenterol*. **1994**, *29* (Suppl. 204), 27−31.
(20) Boucher, E.; Jouanolle, H.; Andre, P.; Ruffault, A.; Guyader, D.; Moirand, R.; Turlin, B.; Jacquelinet, C.; Brissot, P.; Deugnier, Y. *Hepatology* **1995**, *21*, 322−327.
(21) Janiak, M. J.; Small, D. M.; Shipley, G. G.; *Biochemistry* **1976**, *15*, 4575−4580;
(22) Mountcastle, D. B.; Biltonen, R. L.; Halsey, M. J. *Proc. Natl. Acad. Sci. U.S.A.* **1978**, *75*, 4906−4910.
(23) Babbitt, B.; Huang, L.; Freire, E. *Biochemistry* **1984**, *23*, 3920−3926
(24) Cevc, G.; Marsh, D. *Phospholipid Bilayers. Physical Principles and Models*; Wiley: New York, 1987; Chapter 8, pp 231−268.
(25) Marsh, D. *CRC Handbook of Lipid Bilayers*; CRC Press: Boca Raton, FL, 1990; pp 135−158.
(26) McDaniel, R. V.; McIntosh, T. J.; Simon, S. A. *Biochim. Biophys. Acta* **1983**, *731*, 97−108.
(27) Simon, S. A.; McIntosh, T. J. *Biochim. Biophys. Acta* **1984**, *773*, 169−172.
(28) Rowe, E. S.; Campion, J. M. *Biophys. J*. **1994**, *67*, 1888−1895.
(29) Vierl, U.; Lobbecke, L.; Nagel, N.; Cevc, G. *Biophys. J*. **1994**, *67*, 1067−1079.
(30) Swamy, M. J.; Marsh, D. *Biophys. J*. **1995**, *69*, 1402−1408.
(31) (a) Levin, I. W.; Tomellini, S. Unpublished Raman spectroscopic data. (b) O'Leary, T. J.; Levin, I. W. *Biochim. Biophys. Acta* **1984**, *776*, 185−189.
(32) Igimi, H.; Carey, M. C. J. *Lipid Res*. **1980**, *21*, 72−90.
(33) Roda, A.; Minutello, A.; Angellotti, M. A.; Fini, A. J. *Lipid Res*. **1990**, *31*, 1433−1443.
(34) Moroi, Y.; Kitagawa, M.; Itoh, H. J. *Lipid Res*. **1992**, *33*, 49−53.
(35) Lee, A. G. Biochim. *Biophys. Acta* **1978**, *514*, 95−104.
(36) Albon, N.; Sturtevant, J. M. *Proc. Natl. Acad. Sci. U.S.A.* **1978**, *75*, 2258−2260.
(37) Craig, N. C.; Bryant, G. J.; Levin, I. W. *Biochemistry* **1987**, *26*, 2449−2458.
(38) Suezaki, Y.; Tatara, T.; Kaminoh, Y.; Kamaya, H.; Ueda, I. *Biochim. Biophys. Acta* **1990**, *1029*, 143−148.
(39) Inoue, T.; Tasaka, T.; Shimozawa, R. *Chem. Phys. Lipids* **1992**, *63*, 203-212.
(40) Prigogine, I.; Defay, R.; Everett, D. H. *Chemical Thermodynamics*; Longmans Green: London, 1954; Chapter 22.
(41) Hill, M. W. *Biochim. Biophys. Acta* **1974**, *356*, 117−124.
(42) Hill, M. W. *Biochem. Soc. Trans*. **1975**, *3*, 149−152.
(43) Sturtevant, J. M. *Proc. Natl. Acad. Sci. U.S.A.* **1982**, *79*, 3963−3967.
(44) Jain, M. K.; Wu, N. M. *J. Membr. Biol*. **1977**, *34*, 157−201.
(45) Donovan, J. M.; Jackson, A. A.; Carey, M. C. *J. Lipid Res*. **1993**, *34*, 1131−1140.
(46) Kuhn-Velten, W. N.; Kempfle, M. A. *Biochim. Biophys. Acta* **1993**, *1145*, 185−190.
(47) Fromherz, P.; Rocker, C.; Ruppel, D. *Faraday Discuss. Chem. Soc*. **1986**, *81*, 39−48.
(48) Jahnig, F. *Biophys. Chem*. **1976**, *4*, 309−318.
(49) Trauble, H.; Teubner, M.; Woolley, P.; Eibl, H. *Biophys. Chem*. **1976**, *4*, 319−342.
(50) Cevc, G.; Watts, A.; Marsh, D. *Biochemistry* **1981**, *20*, 4955−4965.
(51) Sperotto, M. M.; Mouritsen, O. G. *Eur. Biophys. J*. **1988**, *16*, 1−10.
(52) Schwarz, F. P. *Thermochim. Acta* **1991**, *177*, 285−303.